Thermal calculation of the radiation chamber of an ethane pyrolysis furnace

D B Vafin[1,6], **A V Sadykov**[1]

[1]Nizhnekamsk Institute of Chemical Technology (branch) Kazan National Research Technological University, Prospect Builders 47, Nizhnekamsk, 423570, Russia

Abstract. Using our own application package that implements the differential method of thermal calculation of furnaces, we calculated the temperature fields in the radiation chamber and the distribution of heat fluxes along the tubular reactors in a ethane pyrolysis furnace. The interconnected combustion processes of fuel gas, the turbulent flow of combustion products, radiant-convective heat transfer are described by two-dimensional equations of transport and motion. Wall burners are installed in eight horizontal rows on both walls of the radiation chamber. The combustion products of fuel gas in the air leaving the nozzles 128 of the burner create complex fields of flow velocities and temperatures in the radiation chamber of the furnace. Heat fluxes to the reaction pipes are formed due to the radiations of flue gases, soot particles and hot lined surfaces of the walls of the combustion chamber.

Pyrolysis furnaces are designed for thermal decomposition of gaseous ethane or butane-propane. Thermal cracking of ethane in tubular reactors of radiation chambers (Figure 1) due to the supply of heat from the products of combustion of fuel gas and hot walls is accompanied by the formation of ethylene, methane, hydrogen and other products.
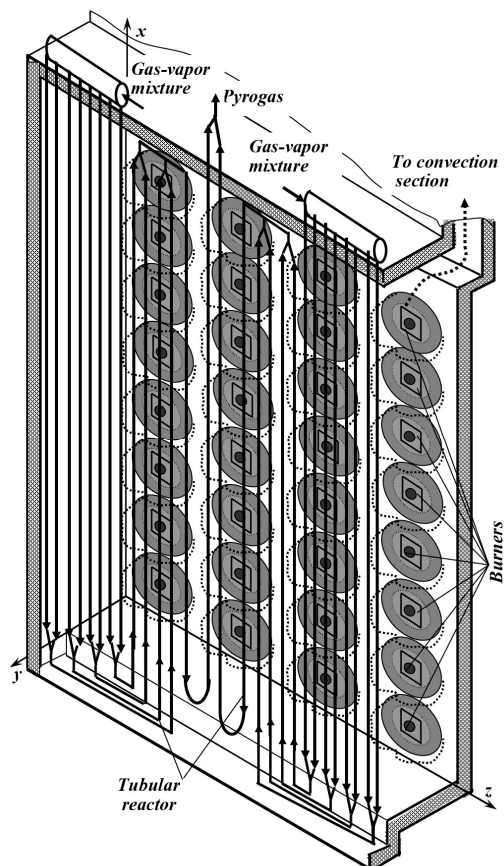
Figure 1. Scheme of the fourth part of radiation chambers of a tubular furnace ethane pyrolysis and coordinate system.

Pyrolysis furnaces consist of convection and radiant sections. During pyrolysis of ethane, with the correct organization of heat supply to the coils of the radiation chamber, ethylene (~48% by weight), hydrogen (~3.51%), and methane are mainly formed. The amount of non-decomposed ethane raw material at the output of the furnace is about 39.4 % by weight. The higher the temperature of the pyrogas at the outlet of the radiant coils of the furnace, the higher the conversion of raw materials. If you deviate from the optimal thermal mode in the radiation chamber, the output of the target product decreases. Therefore, at the design stage of the furnace, it is necessary to choose the correct type of burners and their location, which provides the desired distribution of heat flows along the height of the tubular reactor. This requires a reliable method of heat calculation of furnaces. Until now, designers mostly use integral methods of thermal calculation based on empirical data. In [1], we proposed a differential method for thermal calculation of tubular furnaces based on modeling of interrelated processes occurring in furnaces by differential equations of energy conservation, equations of turbulent gas movement, and an integro-differential equation of energy transfer by radiation. The application of the proposed method for calculating tubular furnaces with multi-tiered wall burners in two-dimensional and three-dimensional calculations is given in [2, 3]. The foundations of this approach to the thermal calculation of furnaces were laid in the work [4]. Various aspects of the application of the differential method of thermal calculation are available in [5-9].

Ethane gas is distributed in four tubular reactors of the radiation chamber in front of the convection section. In the convection section, various streams, including a mixture of hydrocarbon feed and dilution steam before being fed into the radiation chamber, are heated by flue gases. The temperature of the raw material mixture at the inlet to the radiant part for the investigated furnace is about 650 °C, and the temperature of the pyrolysis products (pyrogas) at the outlet of the tubular reactor is 835 °C.

Figure 1 shows one fourth of the radiation chamber of a furnace. The height of the radiation chamber along the x axis is 11 m, the depth along the z axis is 10 m and the width – is 2 m. On the lateral lined walls of the radiation chamber on eight rows are 64 burners on each side of the John Zinc type LPMW-5 with a rated power of 186 kW. The percentage of fuel gas: H_2 – 18.5; CH_4 – 78.35; C_2H_6 – 1.6; N_2 – 1.3; O_2 – 0.25%. In the calculations, the temperature of the fuel gas supplied to the burners is assumed to be 60 °C. The lowest calorific value of the fuel is 29 Mj / nm^3. The temperature of the air supplied to the burners is taken equal to 2 °C. The coefficient of excess air $\alpha = 1.1$.

The differential method of thermal calculation of furnaces is based on concurrent integration of equations: 2D equations of radiative transfer within approximation of discrete ordinate method (1), energy equation (2), turbulent flow of a gas mixture (3), two-parametric $k-\varepsilon$ turbulence model (4), continuity equation and gas state (5), convective-diffusion equation for transfer of air and fuel components (6):

$$\mu_m \frac{\partial I_m^k}{\partial x} + \xi_m \frac{\partial I_m^k}{\partial y} = \alpha_\lambda \int_{\lambda_{k-1}}^{\lambda_k} I_{b\lambda} d\lambda - (\alpha_k + \beta_k) I_m^k + \frac{\beta_k}{4\pi} \sum_{m'=1}^{N_o} w_{m'} \phi_{m'm} I_{m'}^k , \qquad (1)$$

$$\rho\, c_p u \frac{\partial T}{\partial x} + \rho\, c_p \upsilon \frac{\partial T}{\partial y} = \frac{\partial}{\partial x}(\lambda_{ef} \frac{\partial T}{\partial x}) + \frac{\partial}{\partial y}(\lambda_{ef} \frac{\partial T}{\partial y}) + (q_v - \mathrm{div}\mathbf{q_p}), \qquad (2)$$

$$\left. \begin{array}{l} \rho u \dfrac{\partial u}{\partial x} + \rho\upsilon \dfrac{\partial u}{\partial y} = -\dfrac{\partial p}{\partial x} + \dfrac{\partial}{\partial x}(\mu_{ef}(2\dfrac{\partial u}{\partial x} - \dfrac{2}{3}\,\mathrm{div}\,\mathbf{v})) + \dfrac{\partial}{\partial y}(\mu_{ef}(\dfrac{\partial u}{\partial y} + \dfrac{\partial \upsilon}{\partial x})) + f_1, \\[4mm] \rho\, u \dfrac{\partial \upsilon}{\partial x} + \rho\upsilon \dfrac{\partial \upsilon}{\partial y} = -\dfrac{\partial p}{\partial y} + \dfrac{\partial}{\partial x}(\mu_{ef}(\dfrac{\partial u}{\partial y} + \dfrac{\partial \upsilon}{\partial x})) + \dfrac{\partial}{\partial y}(\mu_{ef}(2\dfrac{\partial \upsilon}{\partial y} - \dfrac{2}{3}\,\mathrm{div}\,\mathbf{v})), \end{array} \right\} \qquad (3)$$

$$\frac{\partial}{\partial x}(\rho\, u\phi) + \frac{\partial}{\partial y}(\rho\upsilon\phi) = \frac{\partial}{\partial x}(\Gamma_\phi \frac{\partial \phi}{\partial x}) + \frac{\partial}{\partial y}(\Gamma_\phi \frac{\partial \phi}{\partial y}) + S_\phi , \qquad (4)$$

$$\frac{\partial(\rho u)}{\partial x} + \frac{\partial(\rho \upsilon)}{\partial y} = 0, \qquad p = \frac{\rho}{\mu_{\mathrm{mix}}} RT. \qquad (5)$$

In those equations we use the following notations: I_m^k is the radiation spectral emittance for selected directions $\mathbf{S}_m\{m = 1, N_0\}$, and those vectors are assigned by a set of angular coordinates $\{\mu_m, \xi_m\}$; $I_{b\lambda}(T)$ is the spectral emittance for a black body at temperature T; α_k, β_k are the average spectral coefficients of absorption and scattering; w_m are the weight coefficients [5]; u, υ are the components of velocity $\mathbf{v}$ for combustion products flow along axices x and y; ρ is the density of combustion products; c_p is the isobaric heat capacity; $\lambda_{ef} = \lambda + \lambda_t$ is the coefficient for effective thermal conductivity; p is the pressure, μ_{mix} is the molar mass of the gas mixture; R is the universal gas constant; q_v is the volumetric density of heat sources; div $\mathbf{q}_p$ is the power of radiant flux density; $\mu_{ef} = \mu + \mu_t$ is the effective viscosity; the coefficients of turbulent viscosity and thermal conductivity calculated from formulas: $\mu_t = c_\mu \cdot f_\mu \cdot \rho\, k^2/\varepsilon$, $\lambda_t = c_p\, \mu_t / \mathrm{Pr}_t$; where Pr_t is the turbulent Prandtl number; $f_1 = -\rho g (1 - \beta(T - T_\infty))$ is the mass force, where $\beta = (1/\rho)(\partial\rho/\partial T)$ is the volumetric expansion coefficient; g is the gravity acceleration; $T_\infty = 290$ K is the temperature taken as standard for calculation of buoyancy force; $\phi = \{k, \varepsilon, m_{H_2}\ m_{CH_4}, m_{C_2H_6}, m_{air}\}$; k, ε is the kinetic energy of turbulent pulsations and kinetic energy dissipation rate; S_ϕ is a source term [4]; $\Gamma_\phi = \mu + \mu_t/\sigma_\phi$ is the transfer coefficient in equation (4), and $m_{H_2}, m_{CH_4}, m_{C_2H_6}$ are the mass concentrations of H$_2$, CH$_4$, C$_2$H$_6$; m_{air} are the mass concentrations of air; $S_f = 0,53\rho\, g_f^{1/2}\, \varepsilon/k$ is the rate of chemical reaction of combustion defined from "vortex break" model [4], $g_i = 2,27(\mu_t\, k/(\rho\varepsilon)(\partial m_i/\partial y)^2$ is the root-mean-square pulsation component of fuel, $i = $ H$_2$, CH$_4$, C$_2$H$_6$; $\Gamma_\phi = \mu / \sigma_t$ is the transfer coefficient in equation (4), where σ_t is the Schmidt number. The constants for $k-\varepsilon$ model and expression for f_μ are taken according to recommendations [7]. Equation like (4) works also for m_{air}. The source term in the equation for the mass concentration of oxidizer (air) is found from relation $S_{air} = S_f A$, where A is stoichiometric air ratio for combustion of 1 kg of fuel ($\Gamma_f = \Gamma_{air}$).

A detailed description of the issues of setting boundary conditions for differential equations (1) – (5), features of their discrediting and numerical solution of the system of obtained algebraic equations is available in [1-3] and in our other publications, references to which are contained in these works.

In the radiation chamber of the furnace, in four tubular reactors of pyrolysis, each of which has eight passes, undergo a process of thermal pyrolysis of ethane in the presence of dilution steam. The entrance passage and the next passage of each coil consist of two parallel pipes. The other six passages consist of a single pipe. The exhaust passages of two tubular reactors are connected in pairs to one input line of each of the two quenching and evaporation apparatus.

As noted above, the furnace is equipped with wall-mounted burners with natural thrust, which are supplied with fuel gas and air from the environment. The thermal load of wall-mounted burners is controlled by controlling the fuel gas supply pressure. The nominal overpressure of the gas in front of the burners is ~0.15 MPa. The air supply is regulated by means of air dampers. The draft required to maintain a reduced pressure of ~1.2 kPa in the radiation chamber is created by the smoke pump. In the design calculations from the experience of operating similar furnaces, it is assumed that the burners will provide a uniform temperature distribution of ~1250 °C (~1550 K) in the combustion chamber.

In our calculations, the tubular screen was considered as a wall with an effective degree of blackness of 0.79 [1]. The thickness of the lined walls of the radiation chamber is assumed to be 0.31 m with an effective thermal conductivity of 0.35 W/(m·K). The degree of blackness of the inner surfaces of the walls is 0.67. The temperature of the outer surface of the walls is 40 °C. The losses of heat through the walls were taken into account.

Figure 2 shows a view of the isotherms in the plane passing through the axes of the burners located in the area of the outlet pipes of the coil. Figure 3 shows graphs of changes in the flue gas temperature at different distances from the side wall surface and a graph of the temperature of the inner surface of the lining in the same section.

As can be seen from figure 2 and 3, the assumption of a uniform temperature field in the radiation chamber is not fulfilled. In fact, the temperature field is complex, it also varies along the depth of the furnace along the z axis. In figure 3, the value of the temperature of the flue gases $t_g = 1190$ °C, measured by the standard thermocouple of the operating furnace, is plotted in a triangle.
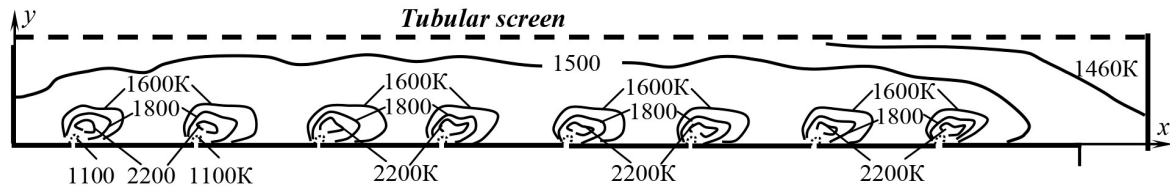
Figure 2. View of isotherms in the radiation chamber of a tubular ethane pyrolysis furnace
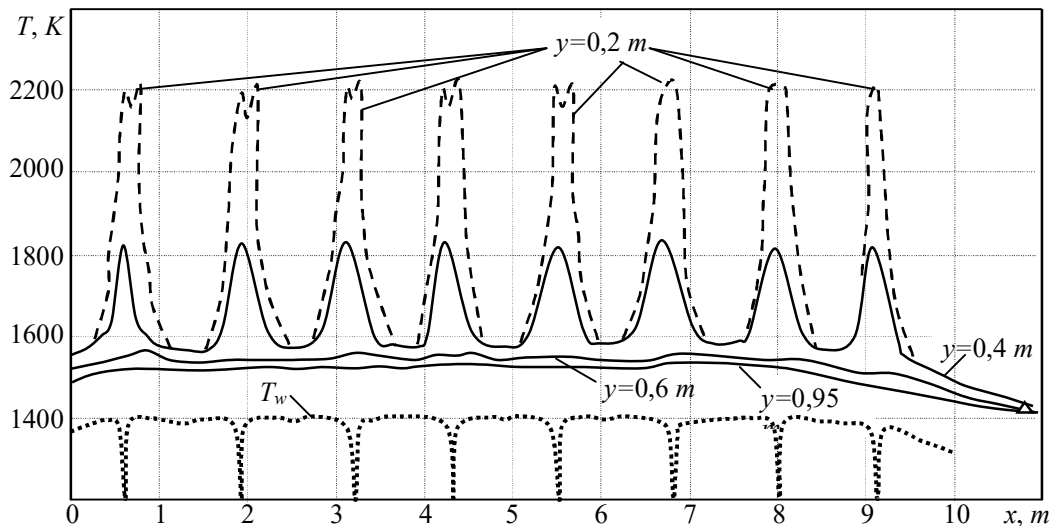
Figure 3. Changes in the temperature of the combustion products at different distances from the side wall (y) and the inner surface of the lining (T_w) along the height of the furnace.

We can see that our calculated values are in good agreement with the experimental value. The lower part of figure 3 shows a graph of changes in the temperature of the inner surface of the side wall of the radiation chamber. It is seen that when using wall burners for volumetric fuel combustion, the wall surface temperature is quite uniform, in contrast to the use of burners that provide combustion along the wall [2, 3].

Figure 4 shows a graph of changes in the surface density of heat flows along the output pipes of the coil in the radiation chamber, where the final reactions of ethane pyrolysis occur at the raw material temperature of ~835°C. When ethane is pyrolyzed, the carbon-carbon bond breaks and two free radicals are formed CH_3:

$$H_3C - CH_3 \rightarrow 2\,CH_3 \quad \text{chain nucleation.}$$

Subsequently, free radicals react with other ethane molecules to form the desired ethylene product. $H_2C = CH_2$ and by-products (methane, acetyline ...):

$$H_3C–CH_3 + CH_3 \rightarrow CH_4 + H_3C–CH_2;\; H_3C + CH_2 + H_2C=CH_2 + H \text{ chain development;}$$

$$H_3C–CH_3 + H \rightarrow H_2 + H_3C–CH_2 ;\; H + H_3C–CH_2 \rightarrow H_3C–CH_3 \text{ open circuit;}$$

$$2(H_3C –CH_2) \rightarrow H_2C=CH_2 + H_3C–CH_3.$$
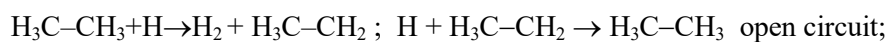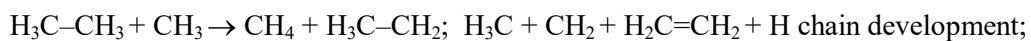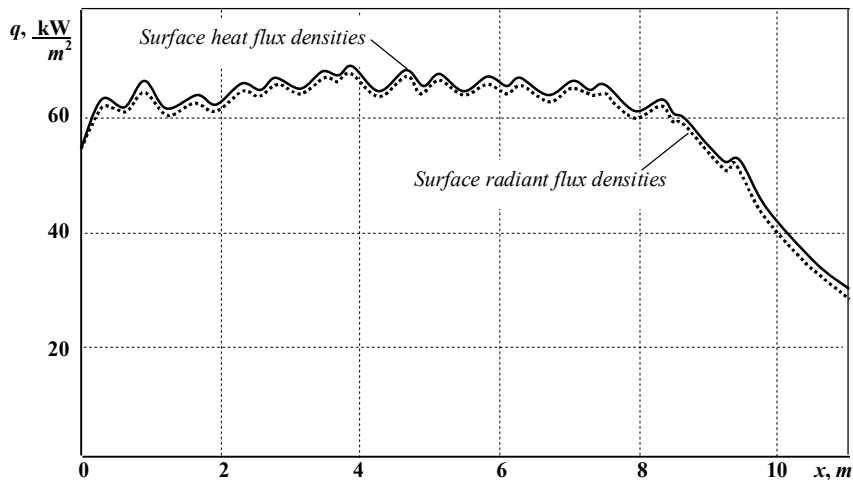
Figure 4. Distribution of surface densities of heat fluxes along the height of the tubular screen.

As can be seen from Figure 4, at low speeds flow rates of the combustion products, the main amount of heat (more than 95%) is transferred to the heated product in tube furnaces due to the radiation of flue gases and incandescent walls. The use of a large number of wall-mounted burners with a multi-tiered arrangement on the side walls (in this case, 8 tiers) provides a fairly uniform thermal stress of the reaction pipes. The lower value of heat fluxes at the bottom of the furnace can be explained with the relatively low temperature of the surface of the furnace bottom. The decrease in heat fluxes in the upper part of the coil tubes is associated with an increase in the temperature of the outer surface of the reaction tubes from 1050 K at the bottom to 1200 K at the top, as well as with a decrease in the temperature of the combustion products towards the exit from the radiation chamber.

According to the calculation results, the heat consumption for heating the raw mixture in the radiation chamber amounted to 2.4 MW; heat consumption for the endothermic reaction of hydrocarbons - 19.33 MW; total useful heat consumption in the radiation chamber is 21.73 MW. These data are in good agreement with the experimental data of the current furnace. Heat losses through the walls of the radiation chamber amounted to 0.35 MW (1.6% of usable heat, which is about 2 times less than in the case of using wall burners with a flat flame near the wall).

Calculations show that even when using a large number of wall burners, it is not possible to ensure a uniform distribution of temperature and heat stress of the coil pipes in the radiation chamber. However, you can achieve the desired composition of the target product by changing the fuel gas consumption. Using our application package, you can analyze various design options of the designed process furnaces in advance, determining local values of temperature and heat flows.

References

[1] Abdullin A M, Vafin D B 1991 Numerical modeling of local heat transfer in the furnaces of tubular ovens, based on differential approximations for radiant heat transfer *J.of Engin. Phys.* **60** 291.
[2] Vafin D B and Sadykov A V 2016. *Thermophysics and Aeromechanics* **23** 2 291.
[3] Vafin D B, Sadykov A V and Butyakov M A 2018 *High Temperature* **56** 4 553.
[4] Pai B R, Michelfelder S and Spalding D B 1978 *Int. J. Heat Mass Transfer* **21** 5 571.
[5] Fiveland W A 1988 *J.of Thermophysics and Heat Transfer* **2** 4 309.
[6] Fiveland W A 1995 *J. Thermophysics and Heat Transfer* **9** 47–53.
[7] Volkov K N 2005 *Thermophysics and Aeromechanics* **12** 3 339–352.
[8] Askarova A S, Bolegenova S A, Maksimov V Y, Bekmukhamet A, Beketaeva M T and Gabitova Z K 2015v*High Temp.* **53** 5 751.
[9] Surzhikov S T 2016 *High Temp.* **54** 2 235.